

## THE SINGLE CRYSTAL STRUCTURE OF NONSTOICHIOMETRIC THALLIUM HEXATITANIUM OCTASELENIDE DETERMINED AT DIFFERENT TEMPERATURES

W.Bensch and J.Koy

Institute for Inorganic Chemistry, University of Frankfurt  
Niederurseler Hang, 6000 Frankfurt a.M. 50, Germany

(Received January 28, 1992; Communicated by P. Hagemuller)

### ABSTRACT

The nonstoichiometric compound  $Tl_xTi_6Se_8$  crystallizes in the hexagonal  $Nb_3Se_4$  structure with Tl atoms located in the hexagonal channels [1,2]. Samples in a wide stoichiometry range have been synthesized and characterized amongst other techniques by single crystal X-ray structures determined sequentially with one crystal. At room temperature the Tl atoms exhibit a very high anisotropic displacement component  $U_{33}$ . It is noteworthy that with decreasing temperature and with decreasing Tl abundance the one dimensional statical disorder increases. In the Tl rich sample the distance within and between Ti-Ti zig zag chains decreases with temperature whereas the opposite trend is observed in the Tl poor sample. The thermal expansion of the lattice is twice as large in the basal  $a_1$ - $a_2$  plane than in the perpendicular direction. Removal of Tl atoms is performed with a chemical redox reaction using  $I_2/CH_3CN$  solutions. It is demonstrated that the lower phase limit is near  $x=0.2$ . The Tl abundance was adjusted in one single crystal used for all structure investigations by this redox reaction. The kinetics is rapid in a first stage and diffusion controlled during subsequent reaction. It is evidenced that the formal valence of the Tl atoms is clearly below +1. Contrary to the isotypic  $Tl_xV_6S_8$  the redox reaction also attacks the titanium selenide host material as seen in SEM micrographs. EDA investigations reveal the microinhomogeneity of the single crystal used for structural studies.

MATERIALS INDEX: Thallium, titanium, selenide

### Introduction

After the pioneering synthesis of the ternary compound  $Tl_xV_6S_8$  [3] a number of isotypic compounds have been prepared [1,4,5]. Whereas

$Tl_xV_6S_8$  seems to be well characterized [3,6-12] only little is known about the other compounds. One of the main features of the  $Nb_3X_4$  structure is the quasi-one-dimensionality of metal zig zag chains running parallel to the crystallographic c-axis. The one-dimensional character is nearly lost in  $Tl_{0.80}Ti_6Se_8$  [11]. No data about the homogeneity range of the title compound are published until now. It is expected that changes within the metal bonding occur both as a function of temperature and composition. In the course of a systematic investigation of the electronic and chemical properties of compounds with the  $Nb_3X_4$  structure the  $Tl_xTi_6Se_8$  system has been synthesized in a wide homogeneity range ( $0.23 < x < 0.80$ ). Samples with  $x < 0.80$  are metastable and are only obtained by a topotactically redox reaction. No crystals with a Tl content  $< 0.2$  were obtained which is attributed to the strong reaction between the host material and the redox agent.

One crystal was selected and structure determinations were performed at several temperatures and various levels of Tl abundance. The Tl content was reduced from the level initially introduced by high temperature synthesis using a chemical reaction involving molecular iodine as precipitation and also as oxidation agent for Tl. This reaction was applied previously to the  $Tl_xV_6S_8$  system [6] where it was thought to act as a "deintercalation" agent for the one dimensional intercalate of ionic  $Tl^+$ . This was shown, however, not to be correct, as the valency of the Tl being much smaller than +1 in  $Tl_xV_6S_8$  [10,12]. The kinetics is complex involving at least two different processes, during the first 60 min about 70 to 80% of the Tl is removed, whereas it takes about another 48 h to reduce the Tl abundance to  $x = 0.03$  [12]. The  $V_6S_8$  host material does not react with the redox agent suggesting that the vanadium sulfide is not implicated in the reaction. It was, however, surprising that the host material of the title compound is heavily attacked by the iodine. This clearly demonstrates that the reactivity of  $Tl_xTi_6Se_8$  is different compared to the isomorphous vanadium compound. The high reactivity is attributed to extensive compositional microinhomogeneities which are detected using EDA. Furthermore, the kinetics seem to be different to that of the vanadium compound. The present contribution focusses onto changes of the crystal structure as a function of temperature and Tl abundance especially onto the disorder of the Tl atoms and to get insight into the host-guest interactions in this valence critical compound. In addition, the chemical reactivity and the microhomogeneity as well as the morphology of this ternary compound were investigated with SEM and EDA.

### Experimental

$Tl_xTi_6Se_8$  ( $x=0.8$ ) was prepared in two different ways: 1. reaction of the elements at 1273 K for 10 days and 2. heat treatment of a mixture of TlSe, Ti and Se at 1400 K for 7 days. The experiments were performed in evacuated and sealed silica ampoules. The variation of temperature and duration of heat treatment do not lead to homogeneous samples. The byproducts were identified as TlSe and small amounts of  $TlTi_6Se_8$ . Removal of Tl was performed using a solution of iodine in acetonitrile (0.5mg  $I_2$ /ml  $CH_3CN$ ). After 25 min reaction time the Tl content was reduced by about 20% leading to the composition  $Tl_{0.65}Ti_6Se_8$ . Subsequent 110 h treatment led to the final com-

position with  $x=0.23$ . After each reaction the single crystal structure was determined. Low temperature X-ray crystal structure determinations were performed to elucidate the reason for the unusual high anisotropic displacement component (ADP)  $U_{33}$ . Scanning electron microscopy (SEM) and energy dispersive analysis (EDA) were applied to characterize the morphology as well as the microhomogeneity of the single crystal under investigation. A number of crystals were investigated to test the significance of the compositional data. EDA data were corrected using the  $\text{SeL}_{\alpha}/\text{SeK}_{\alpha}$  ratio as a measure for absorption and topography effects. Single crystal work was performed on a STOE AED II diffractometer using monochromated  $\text{MoK}_{\alpha}$  ( $\lambda = 0.7107 \text{ \AA}$ ) radiation. SEM and EDA investigations were performed with a JEOL JSM-35 equipped with an ORTEC EDA system. The base pressure within the microscope was about  $10^{-6}$  torr.

### Results and Discussion

Single crystal structure determination: The main features of the crystal structure are triple chains of face sharing  $\text{TiSe}_6$  octahedra which are connected by common edges leading to a three dimensional network with large hexagonal channels parallel to the  $c$ -axis. The Tl atoms are located within the channels. All calculations were performed in the space group  $P6_3/m$  with the program package SHELXTL PLUS [13].

Attempts to refine the crystal structure in the acentric space group  $P6_3$  gave no better results. A numerical absorption correction was performed for all crystals. The relatively high internal  $R$ -values of the datasets of the Tl poor compound are due to the macroscopic damage of the crystal during the chemical reaction (see below).

In all cases the Tl content of the crystal was determined in the following way: the host lattice  $\text{Ti}_6\text{Se}_9$  was first refined isotropically. The Tl atoms are placed at the highest difference electron density peaks, i.e. at 0,0,0 for  $x=0.8$  and 0.65 and at 0,0,0.12 for  $x=0.23$ . Then the refinement was performed with a free varying site occupation factor (SOF) for Tl. The final Tl contents obtained in this way are 0.80(4), 0.65(4) and 0.23(4), respectively. The results of the crystal structure refinements and essential technical details are summarized in Table 1. The reason for the large standard deviations is the high correlation between the  $z$ -coordinate, the  $U_{1s}$  and the SOF.

$\text{Tl}_{0.8}\text{Ti}_6\text{Se}_9$ : In general the obtained structural parameters are in good agreement with those published by [1]. The thermal expansion of the crystallographic  $a$ -axis is two times larger than that of the  $c$ -axis. This indicates that the lattice is more rigid parallel to the  $c$ -axis due to repulsive interactions between neighbored Tl atoms within the channel.

The refinement with Tl at 0,0,0 leads to an  $U_{33}$  for the Tl atom of 0.78(16), indicative for high thermal vibrations or static disorder. With decreasing temperature the  $U_{33}$  is reduced by about 35% to 0.51(5). Calculations with splitted Tl sites or with Tl at different  $z$ -coordinates led to no better results or to clearly higher  $U_{33}$  components ( $U_{33} = 1.96(56)$  for  $z=0.25$ ). The refinement

TABLE 1  
Refinement results for  $\text{Tl}_x\text{Ti}_6\text{Se}_8$  ( $x=0.80, 0.64$  and  $0.23$ ).

Temperature [K]	295	200	170	100
a [Å]	9.8853(6)	9.8754(5)	9.8734(5)	9.8669(8)
c [Å]	3.5957(3)	3.5912(3)	3.5901(3)	3.5876(4)
Volume	304.30	303.30	303.09	302.48
c/a	0.364	0.364	0.364	0.364
2 $\theta$ range	3-50	3-50	3-50	3-50
$\Sigma I$	677	677	677	677
unique data	215	215	214	214
$R_{\text{int}}$ [%]	2.11	1.79	1.83	1.66
$\mu$ [ $\text{mm}^{-1}$ ]	35.88	36.00	36.02	36.09
y in weight <sup>1</sup>	0.00068	0.0015	0.0015	0.0015
Extinction $g^2$	0.011(1)	0.0034(8)	0.0028(8)	0.0020(7)
Data used [ $F > 2\sigma(F)$ ]	206	208	206	207
$\delta F$ [ $e/\text{\AA}^3$ ]	0.91	1.19	1.05	1.22
	-0.93	-1.69	-1.27	-1.45
R(F) [%]	2.69	3.10	2.79	3.05
Rw(F) [%]	2.66	3.58	3.42	3.82
GOOF	1.28	1.45	1.47	1.55
Tl $\text{U}_{33}$ [ $\text{\AA}^2$ ]	0.78(16)	0.62(9)	0.59(7)	0.51(5)
Tl $\text{U}_{33}/\text{U}_{11}$	18.3	17.4	17.7	20.9
thermal expansion a-axis		9.454 $10^{-5}$		
thermal expansion c-axis		4.194 $10^{-5}$		

**Tl<sub>0.64</sub>Ti<sub>6</sub>Se<sub>8</sub>****Tl<sub>0.23</sub>Ti<sub>6</sub>Se<sub>8</sub>**

T [K]	295	295	100
a [Å]	9.885(1)	9.883(1)	9.858(2)
c [Å]	3.597(1)	3.591(1)	3.577(1)
Volume [ $\text{\AA}^3$ ]	304.36	303.75	301.1
c/a	0.364	0.363	0.363
2 $\theta$ range	3-50	3-50	3-55
$\Sigma I$	680	681	919
unique data	215	215	270
$R_{\text{int}}$ (%)	3.41	4.74	8.24
$\mu$ ( $\text{mm}^{-1}$ )	33.74	28.34	28.59
y in weight <sup>1</sup>	0.00113	0.00005	0.00035
Extinction $g^2$	0.0053(6)	0.0019(3)	-
Data used [ $F > 4\sigma(F)$ ]	192	198	192
$\delta F$ [ $e/\text{\AA}^3$ ]	1.00	1.7	3.12
	-0.79	-1.36	2.03
R(F) [%]	2.36	4.28	5.06
Rw(F) [%]	2.29	3.28	3.90
GOOF	0.88	1.78	1.16
Tl $\text{U}_{33}$ [ $\text{\AA}^2$ ]	0.71(11)	0.11(7)	0.03(1)
Tl $\text{U}_{33}/\text{U}_{11}$	17.5	5.0	10.2
thermal expansion a-axis		1.289 $10^{-4}$	
thermal expansion c-axis		7.217 $10^{-5}$	

<sup>1</sup> weighting scheme:  $w=1/(\sigma^2(F) + yF^2)$ <sup>2</sup> extinction coefficient in  $F^*=F_c/(1+0.002xgxF_c^2/\sin 2\theta)^{1/4}$

with a free varying  $z$ -coordinate led to  $z=0.123(1)$  and an  $U_{33}$  of  $0.12(1)$ . The obtained  $z$  parameter is exactly located between the two special coordinates 0.0 and 0.25. The calculated electron density map shown in Fig.1 clearly demonstrates that the highest peak is located at  $z=0.0$  (shown in Fig.1).

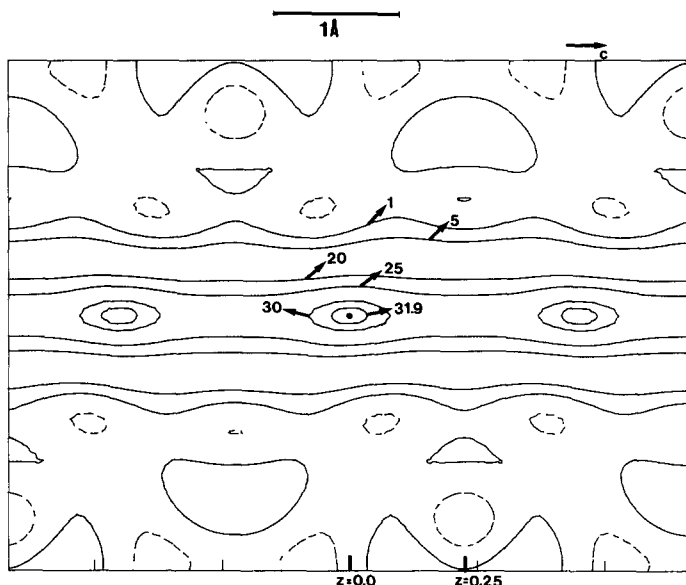


FIG.1

Electron density distribution within the hexagonal channel. Centre of projection 0,0,0. Levels are given in  $e^-/\text{\AA}^3$ .

The decrease of the  $U_{33}$  is reflected in the electron density maps calculated at 295 K and at 100 K. The highest peak is  $31.9 e^-/\text{\AA}^3$  at 295 K and  $39.1 e^-/\text{\AA}^3$  at 100 K.

If the observed  $U_{33}$  component would be due to thermal vibrations its value should tend to zero when extrapolating to 0 K. As can be seen from Fig.2 the Tl  $U_{33}$  vs.  $T$  curve does not intersect the  $U_{33}$ -axis near zero within the margin of error. Furthermore, the ratio  $U_{33}/U_{11}$  increases with decreasing temperature. The  $U_{11}$  components of the other atoms as well as the  $U_{11}$  of the Tl atom behave, however, as expected. These observations suggest that the Tl atoms are one-dimensionally disordered within the hexagonal channels whereas the host lattice shows no significant disorder. The disorder is larger at 100 K than at 295 K.

At  $z=0.00$  the Tl atoms are in a regular trigonal antiprismatic environment with a Tl-Se(1) distance of  $3.360(1)$  Å. This distance is smaller than the sum of the ionic radii of  $\text{Tl}^+$  and  $\text{Se}^{2-}$  ( $1.50$  Å for  $\text{Tl}^+$  and  $1.93$  Å for  $\text{Se}^{2+}$ ) indicative for a partially covalent character of the Tl-Se bond. In other ternary Tl containing transition metal selenides with the stoichiometry  $\text{Tl}_x\text{T}_3\text{Se}_8$  ( $T=\text{Ti}, \text{V}, \text{Cr}$ ;  $x$  near 1) the Tl-Se bond lengths vary from  $3.344$  to  $3.635$  [14]. It should be noted that in the isostructural compound  $\text{Tl}_{0.78}\text{V}_6\text{Se}_8$  the

Tl atoms are in a trigonal planar environment which was attributed to the highly covalent character of the Tl-S bond [12].

Some important bond distances are summarized in Table 2. The average Ti-Se distance changes only little between RT (2.596(2) Å) and 100 K (2.592(3) Å). The difference  $\text{Ti-Se}_{\text{max}} - \text{Ti-Se}_{\text{min}}$  decreases from 0.099 Å at RT to 0.091 Å at 100 K indicative for less distorted  $\text{TiSe}_6$  octahedra. At 100 K, the distance within the Ti-Ti zig-zag chains parallel to the c-axis (3.224(3) Å) is 1.74 % shorter than between the chains (3.280(2) Å; distance in Ti metal: 2.896 Å). With decreasing temperature the Ti-Ti<sub>intra</sub> separation remains constant (3.224(5) Å at 100 K), whereas the inter-chain distance decreases to 3.271(3) Å. This results in a less pronounced anisotropy at 100 K (see Table 2).

TABLE 2  
Important bond distances (Å) in  $\text{Tl}_{0.80}\text{Ti}_6\text{Se}_8$  and  
 $\text{Tl}_{0.23}\text{Ti}_6\text{Se}_8$

$\text{Tl}_{0.80}\text{Ti}_6\text{Se}_8$

T[K]	295	200	170	100
Tl-Se1 (6x)	3.360(1)	3.357(1)	3.356(1)	3.354(1)
Ti-Se2 (2x)	2.611(1)	2.608(2)	2.608(1)	2.605(2)
Ti-Se1 (2x)	2.562(1)	2.560(2)	2.559(2)	2.560(2)
Ti-Se1	2.571(3)	2.571(4)	2.571(4)	2.568(4)
Ti-Se1	2.661(3)	2.654(4)	2.654(4)	2.651(4)
<Ti-Se>	2.596	2.594	2.593	2.592
$\text{Ti-Se}_{\text{max}} - \text{Ti-Se}_{\text{min}}$	0.099	0.094	0.095	0.091
Ti-Ti <sub>intra</sub>	3.224(3)	3.226(5)	3.225(5)	3.224(5)
Ti-Ti <sub>inter</sub>	3.280(2)	3.275(3)	3.276(3)	3.271(3)
Anisotropy [%]	1.74	1.52	1.58	1.46

$\text{Tl}_{0.23}\text{Ti}_6\text{Se}_8$

T[K]	295	100
Tl-Se1 (3x)	3.273(5)	3.268(2)
Tl-Se1 (3x)	3.517(13)	3.494(5)
Ti-Se2 (2x)	2.611(1)	2.606(2)
Ti-Se1 (2x)	2.555(2)	2.547(2)
Ti-Se1	2.581(4)	2.569(4)
Ti-Se1	2.643(4)	2.640(4)
<Ti-Se>	2.593	2.586
$\text{Ti-Se}_{\text{max}} - \text{Ti-Se}_{\text{min}}$	0.088	0.093
Ti-Ti <sub>intra</sub>	3.243(5)	3.223(5)
Ti-Ti <sub>inter</sub>	3.285(3)	3.282(3)
Anisotropy [%]	1.3	1.83

In contrast, in the isostructural compound  $\text{Tl}_x\text{V}_6\text{S}_8$  the anisotropy is larger at 100 K than at 295 K [12].

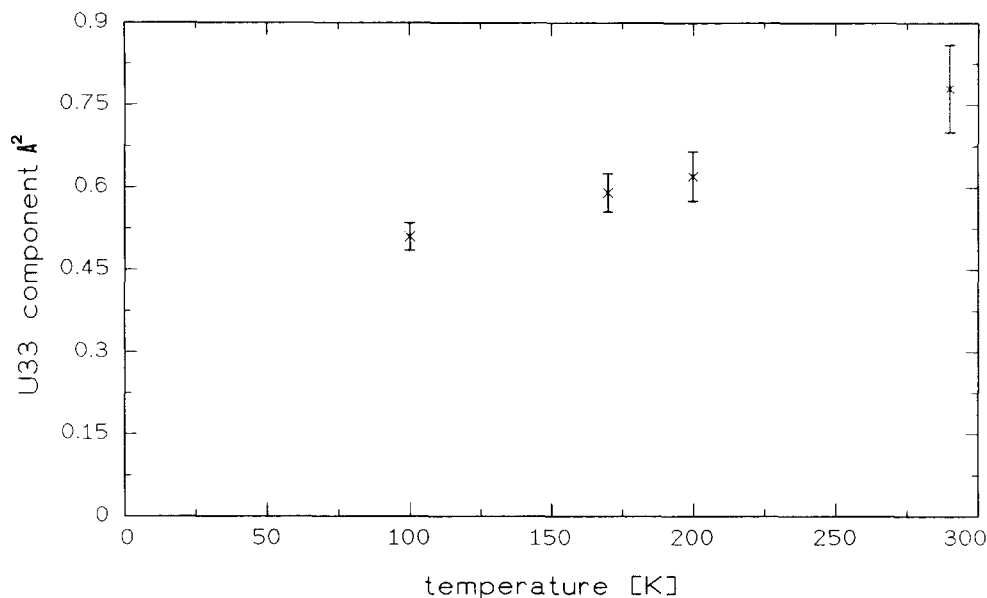


FIG.2

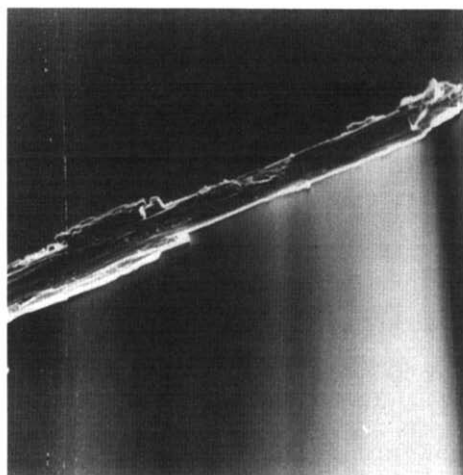
The variation of the anisotropic displacement component  $U_{33}$  of Tl with temperature.

**$\text{Tl}_{0.64}\text{Ti}_6\text{Se}_8$**  : The lattice parameters as well as the  $c/a$  ratio are identical to those obtained for the Tl rich compound. The  $U_{33}$  component of Tl reaches 0.71(11) with Tl at  $z=0.00$ . Attempts to refine the Tl atoms at different  $z$ -positions yielded comparable results as described for  $\text{Tl}_{0.8}\text{Ti}_6\text{Se}_8$ .

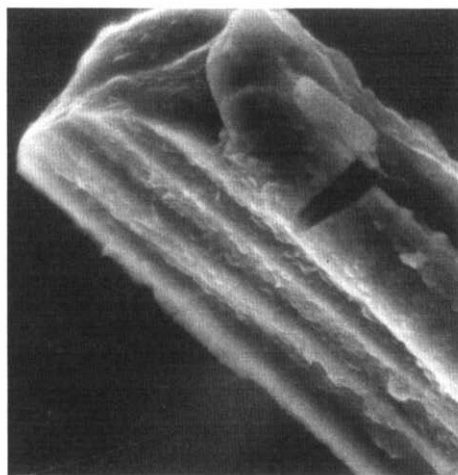
**$\text{Tl}_{0.23}\text{Ti}_6\text{Se}_8$**  : As can be seen from table 1 the lattice parameters change only slightly compared to the Tl rich compound. As in the Tl rich compound the thermal expansion of the lattice is markedly anisotropic. The absolute reduction of the  $c$ -axis with temperature is significantly larger than in the Tl rich sample. This may be explained with the lower occupation density within the channel in  $\text{Tl}_{0.23}\text{Ti}_6\text{Se}_8$  and hence less repulsive interactions between neighboured Tl atoms. After refinement of the host matrix  $\text{Ti}_6\text{Se}_8$  the highest difference electron density peak was found at 0 0 0.12, where Tl was placed. In the final stages of the refinement the  $z$ -coordinate was allowed to vary freely resulting in an  $U_{33}$  component at 300 K of 0.11(7). Refinements with Tl fixed at  $z=0.0$  led to an  $U_{33}$  of 0.46(11), with Tl at  $z=0.25$  the  $U_{33}$  component was 1.66(60). The  $U_{33}$  component significantly decreases with decreasing temperature reaching 0.03(1) at 100 K. Nevertheless, taking advantage of the ratio  $U_{33}/U_{11}$  the disorder is more distinct at 100 K.

The  $\text{TiSe}_6$  octahedra seem to be less distorted compared to the Tl-rich compounds (see Table 2). The environment of the Tl atoms can be described as distorted trigonal antiprism with 3 Tl-Se bonds being markedly shorter than the other three contacts. At 295 K the  $\text{Ti-Ti}_{\text{intra}}$  separation is only 1.3% smaller than the  $\text{Ti-Ti}_{\text{inter}}$  distance, the absolute value of the intra bonds being larger than in the Tl rich compound. Contrary to  $\text{Tl}_{0.23}\text{Ti}_6\text{Se}_8$  the anisotropy significantly increases with decreasing temperature.

**EDA/SEM investigations:** Ohtani *et al.* have reported that Tl may completely be removed from the isotypic compound  $\text{Tl}_x\text{V}_6\text{S}_8$  [6]. A more rigorous investigation revealed that no crystals free of Tl can be obtained even after long reaction times or with boiling agent [12]. Further investigations gave evidence that the topotactic "deintercalation" is better described by a combination of a redox reaction and a deintercalation [15]. In Fig.3 SEM micrographs are shown of the crystal used for the structure determinations with the composition  $\text{Tl}_{0.23}\text{Ti}_6\text{Se}_8$ . Even at low magnification the macroscopic damage of the crystal is clearly seen. Higher magnifications reveal deep reefs running parallel to the needle axis due to preferred chemical etching of the substrate.



12um



2um

FIG.3

SEM micrographs of the crystal with the composition  $\text{Tl}_{0.23}\text{Ti}_6\text{Se}_8$ .

The overall morphology of the crystal is strongly inhomogeneous. This observations suggest that the chemical reaction between  $\text{I}_2/\text{CH}_3\text{CN}$  not only removes the Tl from the channels but also reacts with the host material. To elucidate whether the morphological inhomogeneity is also reflected in the chemical composition point to point elemental analysis were performed. The EDA results in-

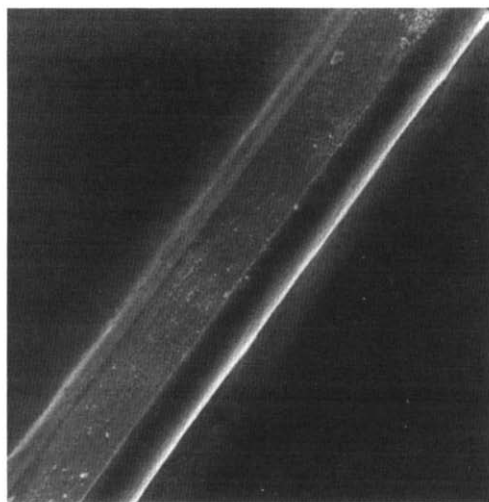


diccate large variations in the composition (see Table 3). At the top of the crystal only little Tl is present which increases towards the seed-end.

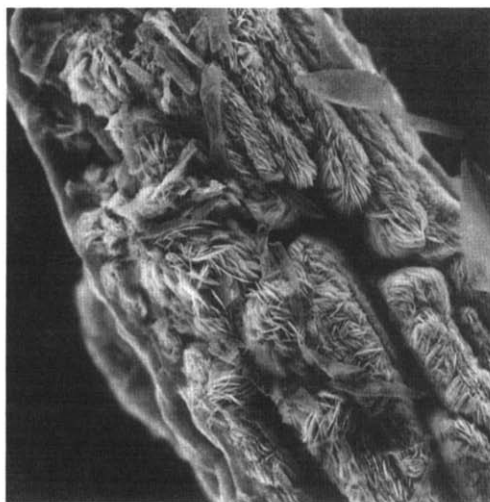
TABLE 3  
Results of the EDA point to point analysis of the crystal  $Tl_{0.23}Ti_6Se_8$ . The overview acts as reference.

	T1	T2	M	B
Ti	1	1	1	1
Se	0.80	0.82	0.52	0.64
Tl	1.10	1.19	1.47	1.97

For comparison other crystals were investigated before and after the reaction with a solution of 0.5 mg  $I_2$ /ml  $CH_3CN$ . Fig.4 shows SEM micrographs of crystals before and after the treatment. The genuine crystals exhibit a smooth surface, but "deintercalation" produces pronounced features leading to a preferential etching of the mosaic structure of the single crystal. Small grains as well as pits are oriented parallel to the needle axis suggesting that selective etching of highly disordered sites within the whole material occurs. The development of the mosaic pattern reflects uneven elemental distribution and/or uneven distribution of lattice defects indicating the microinhomogeneity of the crystal. The flower-like agglomerates which are mainly composed of Se indicate the presence of V-poor Tl-selenide within the material exhibiting a homogeneous morphology before "deintercalation".



17μm



9μm

FIG.4  
SEM micrographs of  $Tl_xTi_6Se_8$  before (left) and after (right) the reaction with  $I_2$  in  $CH_3CN$ .

### Conclusion

Metastable derivatives of the nonstoichiometric title compound can be obtained by a chemical leaching procedure with the lower phase limit extended down to  $x=0.23$  in  $Tl_xTi_6Se_8$ . Samples with  $x<0.2$  could not be obtained due to a strong reaction between the redox agent and the host material. The Ti-Ti bonding properties are significantly influenced by both the temperature and Tl abundance. Whereas in the Tl rich sample the "one-dimensionality" of the Ti-Ti bonds decreases with decreasing temperature the opposite trend is observed in the Tl poor compound. These observations let us speculate that the electrical conductivity as a function of temperature parallel to the c-axis should exhibit pronounced differences between these two compounds. Unfortunately, single crystals suitable for resistivity measurements are not available until yet. Further work is in progress to prepare such crystals. In all compounds the Tl atoms are disordered within the hexagonal channels. The disorder is static with its exact origin remaining speculative. The disorder increases with decreasing temperature. The change of the averaged Tl position is accompanied by a small increase of the charge of the Tl atoms towards a more "ionic" character as could be demonstrated for the isotypic compound  $Tl_xV_6S_8$  [12]. We suppose that the same effects occur also here caused by the variation of the Tl abundance. SEM and EDA gave evidence that the reaction of  $Tl_xTi_6Se_8$  with  $I_2/CH_3CN$  is best described as a redox reaction in which the host lattice is involved. It is not a simple intercalation-deintercalation reaction couple. The high reactivity is attributed to extensive microinhomogeneities which was manifested by SEM and EDA investigations.

Acknowledgements: Financial support by the Deutsche Forschungsgemeinschaft DFG and helpful discussions with R.Schlögl are gratefully acknowledged.

### References

- 1 H.Boller, K.Klepp, Mat.Res Bull. **18**, 437 (1983)
- 2 J.G.Smeggil, J.Solid State Chem. **3**, 248 (1971)
- 3 M.Vlasse, L.Fournes, Mat.Res.Bull. **11**, 1527 (1976)
- 4 R.Schöllhorn, W.Schramm, D.Fenske, Angew.Chem. **92**, 477 (1980)
- 5 T.Ohtani, S.Onoue, Mat.Res.Bull. **21**, 69 (1986)
- 6 T.Ohtani, S.Onoue, J.Solid State Chem. **59**, 324 (1985)
- 7 H.Nishihara, T.Ohtani, S.Onoue, Europhys. Lett. **8**, 189 (1989)
- 8 H.Nishihara, S.Onoue, T.Ohtani, H.Yasuoka, J.Magn.Magn.Mater. **70**, 225 (1987)
- 9 H.Eckert, W.Müller-Warmuth, W.Schramm, R.Schöllhorn, Solid State Ionics, **13**, 1 (1984)
- 10 R.Schlögl, W.Bensch, J.Less-Common Met. **132**, 155 (1987)
- 11 W.Bensch, J.Abart, E.Amberger, Solid State Comm. **58**, 631 (1986)
- 12 W.Bensch, J.Koy, M.Wesemann, J.Less-Common Met., in press
- 13 SHELXTL Plus, Integrated hardware/software package for crystal structure determination, Siemens Analytical X-ray Instruments, 1990
- 14 K.Klepp, H.Boller, J.Solid State Chem. **48**, 388 (1983)
- 15 W.Bensch, J.Koy, E.Wörner, in preparation